US012393091B2

(12) **United States Patent**
Doerr

(10) **Patent No.: US 12,393,091 B2**
(45) **Date of Patent: Aug. 19, 2025**

(54) **TRANSVERSE-MAGNETIC POLARIZATION SILICON-PHOTONIC MODULATOR**

(71) Applicant: **Aloe Semiconductor Inc.**, Irvine, CA (US)

(72) Inventor: **Christopher R. Doerr**, Irvine, CA (US)

(73) Assignee: **Aloe Semiconductor Inc.**, Middletown, NJ (US)

(*) Notice: Subject to any disclaimer, the term of this patent is extended or adjusted under 35 U.S.C. 154(b) by 0 days.

(21) Appl. No.: **18/667,145**

(22) Filed: **May 17, 2024**

(65) **Prior Publication Data**

US 2025/0123534 A1 Apr. 17, 2025

Related U.S. Application Data

(63) Continuation of application No. 17/529,321, filed on Nov. 18, 2021, now Pat. No. 12,001,118.

(51) **Int. Cl.**

G02F 1/225	(2006.01)
G02B 6/12	(2006.01)
G02B 6/122	(2006.01)
G02F 1/21	(2006.01)

(52) **U.S. Cl.**

CPC ***G02F 1/2257*** (2013.01); ***G02B 6/122*** (2013.01); ***G02F 1/212*** (2021.01); *G02B 2006/12061* (2013.01); *G02B 2006/12097* (2013.01); *G02B 2006/12142* (2013.01)

(58) **Field of Classification Search**

CPC G02F 1/2257; G02F 1/212; G02F 1/025; G02B 6/122; G02B 2006/12061; G02B 2006/12097; G02B 2006/12142

See application file for complete search history.

(56) **References Cited**

U.S. PATENT DOCUMENTS

9,235,068	B2	1/2016	Manouvrier
9,529,150	B2	12/2016	Orcutt et al.
9,625,746	B2	4/2017	Chen et al.
10,554,014	B1	2/2020	Doerr et al.
10,996,539	B2	5/2021	Takahashi et al.
11,543,728	B2	1/2023	Doerr

(Continued)

OTHER PUBLICATIONS

Doerr et al., "Silicon Photonics in Optical Coherent Systems," Proceedings of the IEEE, Dec. 2018, 106(12):2291-2301.

(Continued)

Primary Examiner — John Bedtelyon
(74) *Attorney, Agent, or Firm* — Fish & Richardson P.C.

(57) **ABSTRACT**

A silicon-photonic optical modulator includes at least one optical input and at least one optical waveguide that is connected to the at least one optical input. The at least one optical waveguide is configured to propagate quasi-transverse-magnetic (quasi-TM) polarized light, where each of the at least one optical waveguide is configured as a rib waveguide that includes a rib arranged on a slab. The silicon-photonic optical modulator also includes at least one electrode configured to apply at least one electric field to the quasi-TM polarized light in the at least one optical waveguide. In some implementations, a height of the rib waveguide is greater than 0.85 λ/n, where λ is a free-space wavelength of light and n is a refractive index of silicon in the silicon-photonic optical modulator, and a width of the rib waveguide is greater than a thickness of the slab.

20 Claims, 10 Drawing Sheets

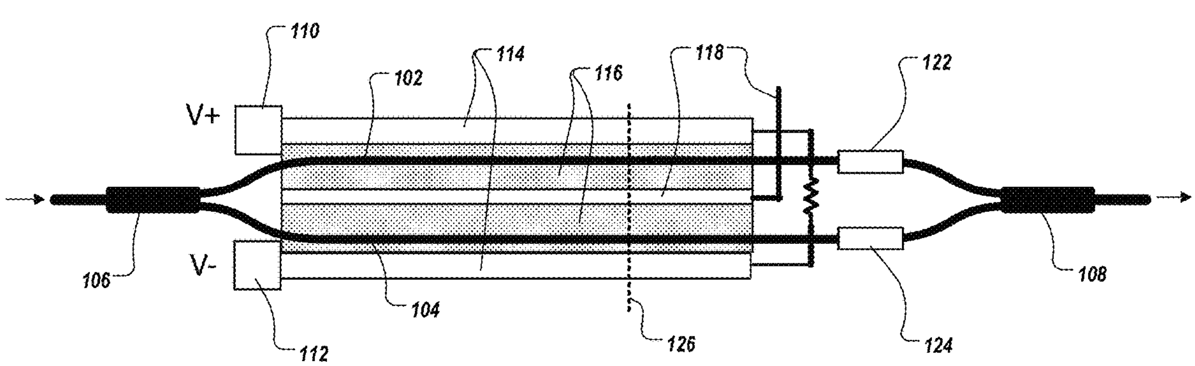

(56) **References Cited**

U.S. PATENT DOCUMENTS

11,586,059	B2 *	2/2023	Simard	G02F 1/025
11,940,709	B2	3/2024	Doerr	
12,001,118	B2	6/2024	Doerr	
2014/0086595	A1	3/2014	Yamazaki	
2022/0326586	A1	10/2022	Doerr	
2023/0145767	A1	5/2023	Doerr	
2023/0152662	A1	5/2023	Doerr	

OTHER PUBLICATIONS

Liow et al., "Silicon modulators and germanium photodetectors on SOI: monolithic integration, compatibility, and performance optimization," IEEE Journal of Selected Topics in Quantum Electronics, Nov. 2009, 16(1):307-315.

Notice of Allowance in U.S. Appl. No. 17/226,730, dated Aug. 31, 2022, 12 pages.

Webster et al., "An efficient MOS-capacitor based silicon modulator and CMOS drivers for optical transmitters," 11th International Conference on Group IV Photonics (GFP), Paris, Aug. 2014, 2 pages.

Witzens, "High-Speed Silicon Photonics Modulators," in Proceedings of the IEEE, Dec. 2018, 106(12):2158-2182.

* cited by examiner

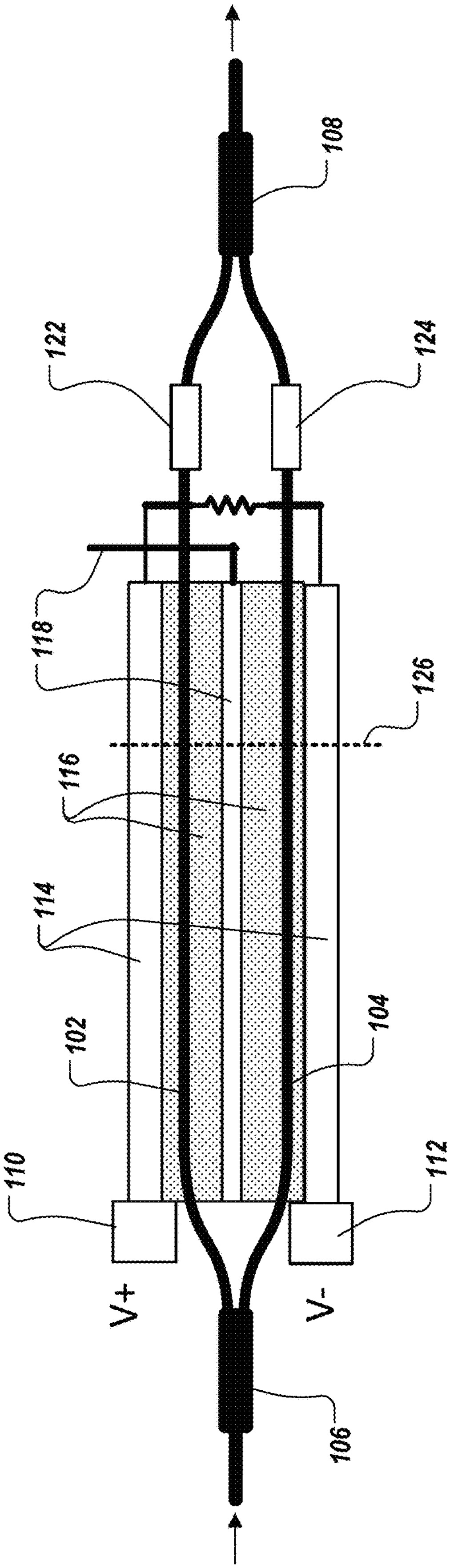

FIG. 1

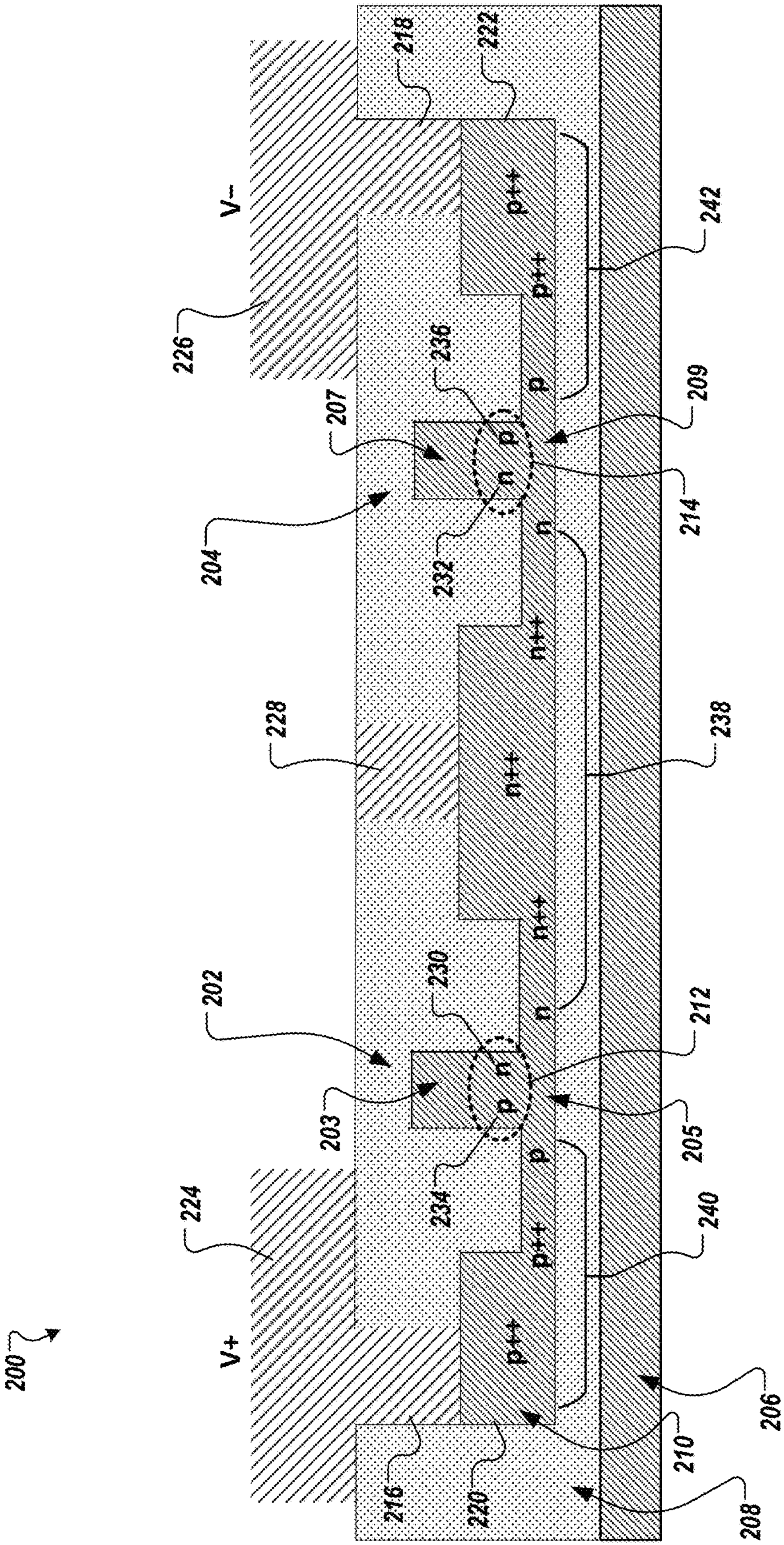
200
V+
V−
224
226
228
202
203
204
207
230
232
234
236
205
209
212
214
216
218
220
222
238
240
242
206
208
210
p++
p++
p
p
n
n
n++
n++
p++
p++
p
p
n
n
n++

FIG. 2

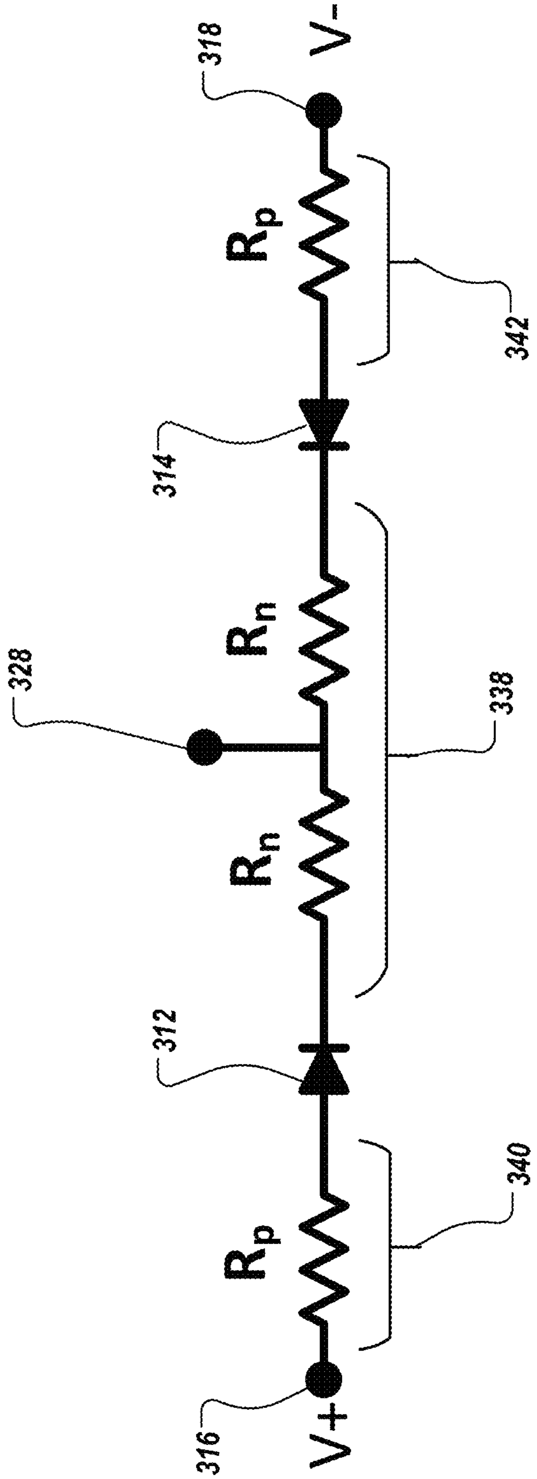

FIG. 3

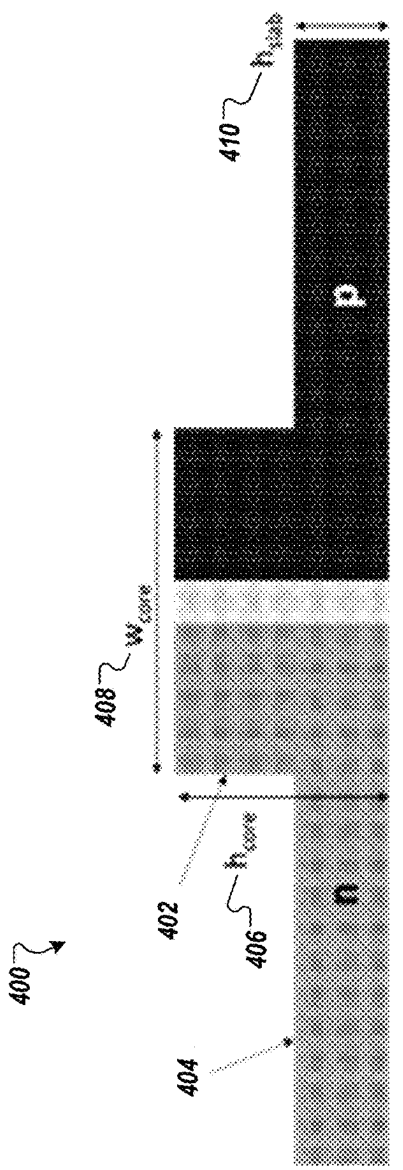
400
402
404
406
408
410
n
p
h_core
w_core
h_slab

FIG. 4A

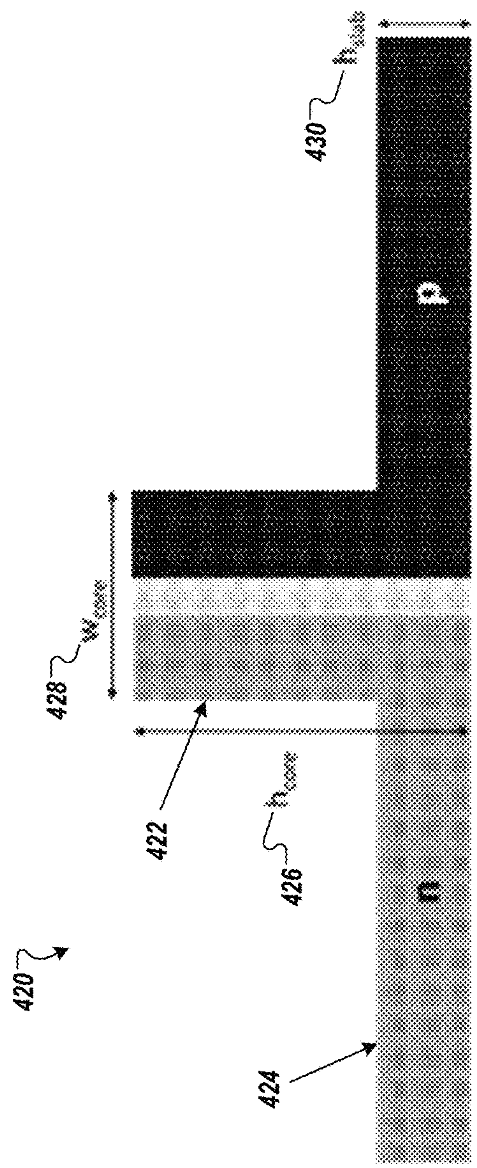
420
422
424
426
428
430
n
p
h_core
w_core
h_slab

FIG. 4B

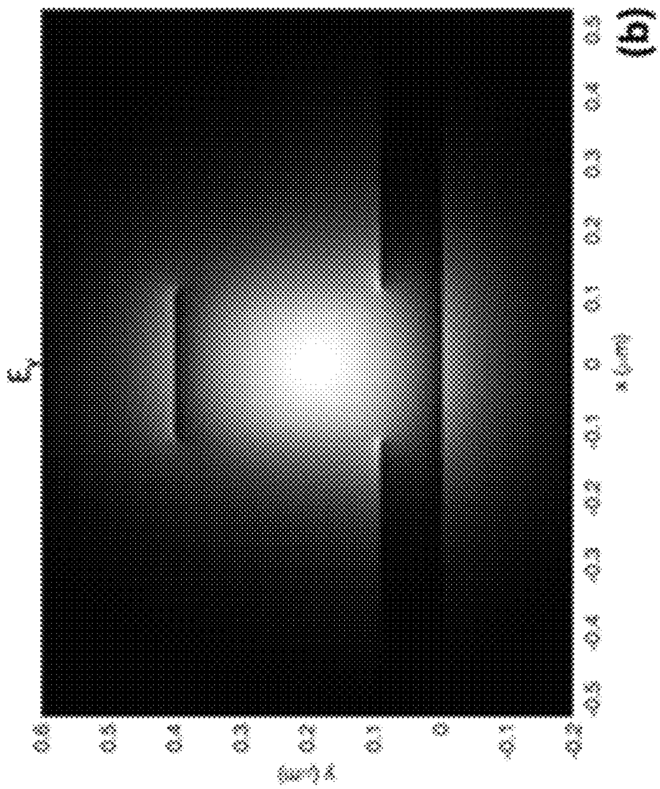

FIG. 5B

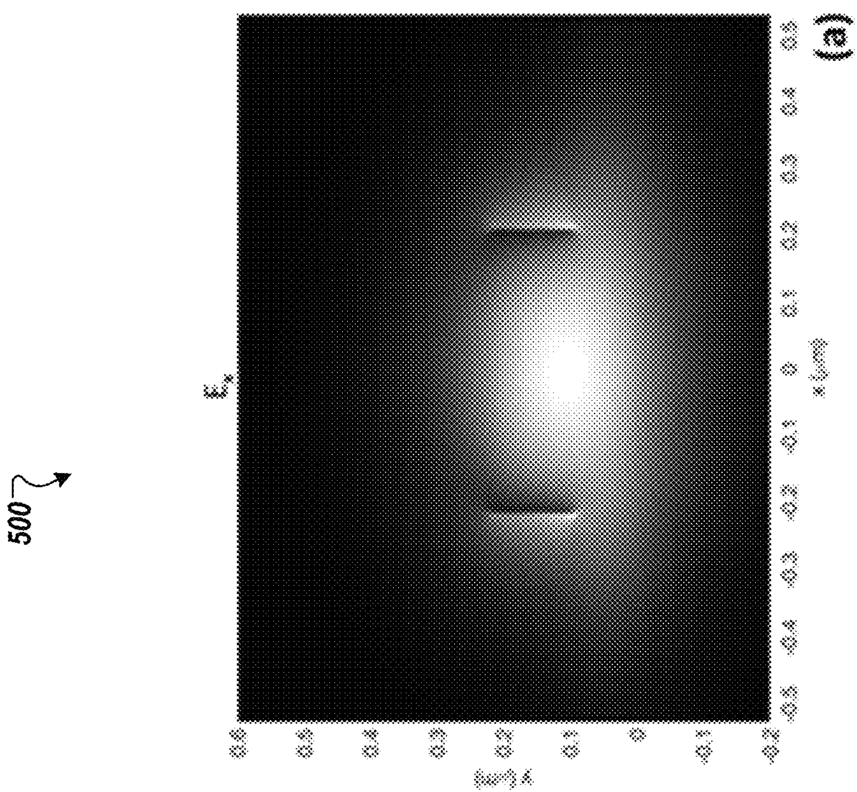

FIG. 5A

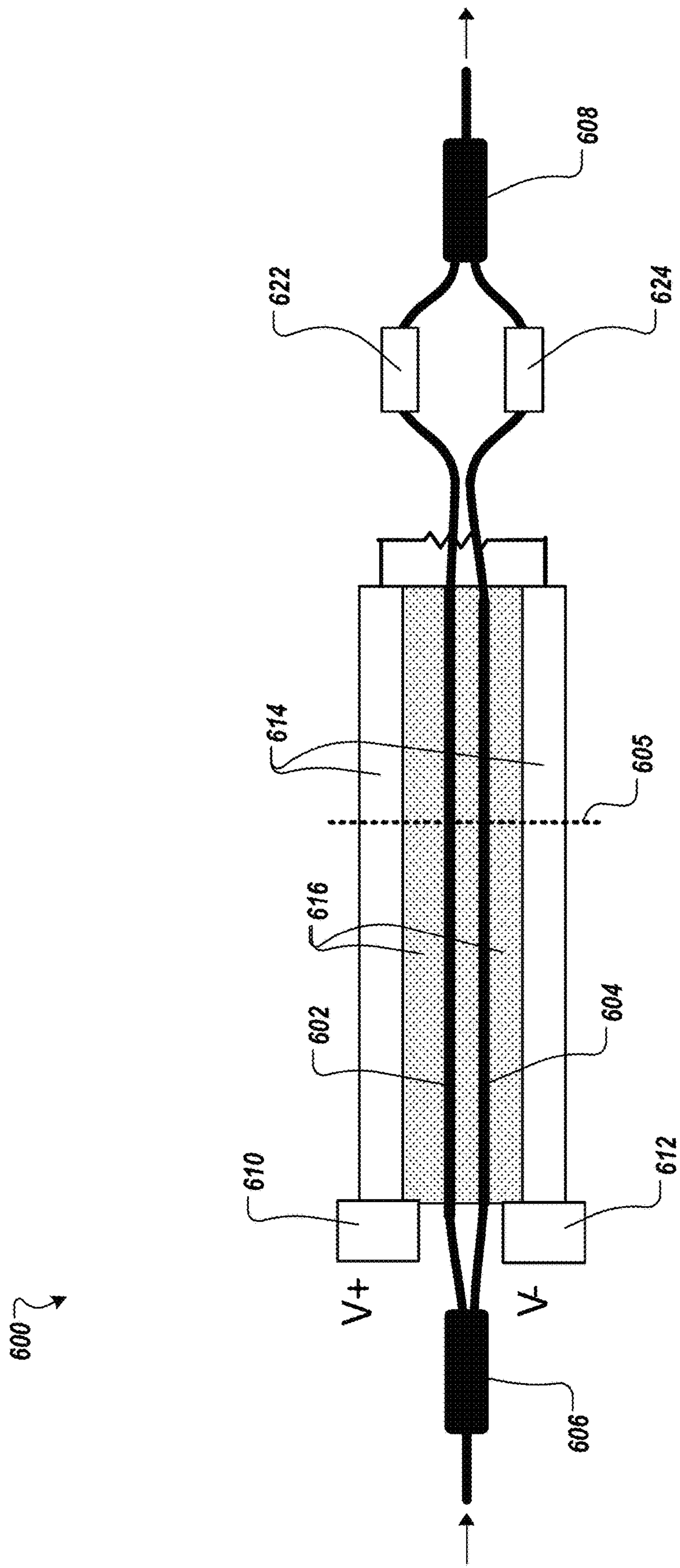

FIG. 6

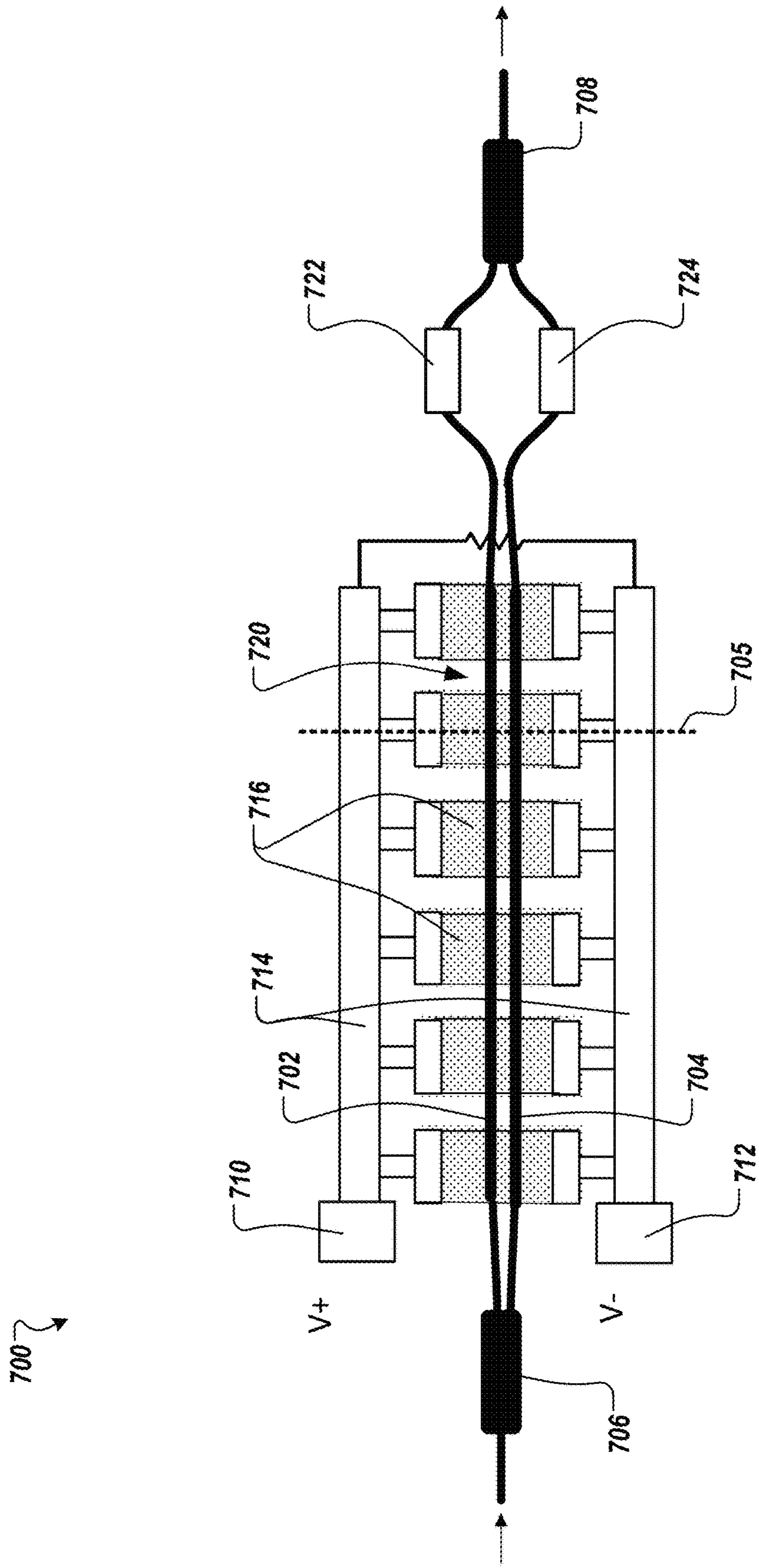

FIG. 7

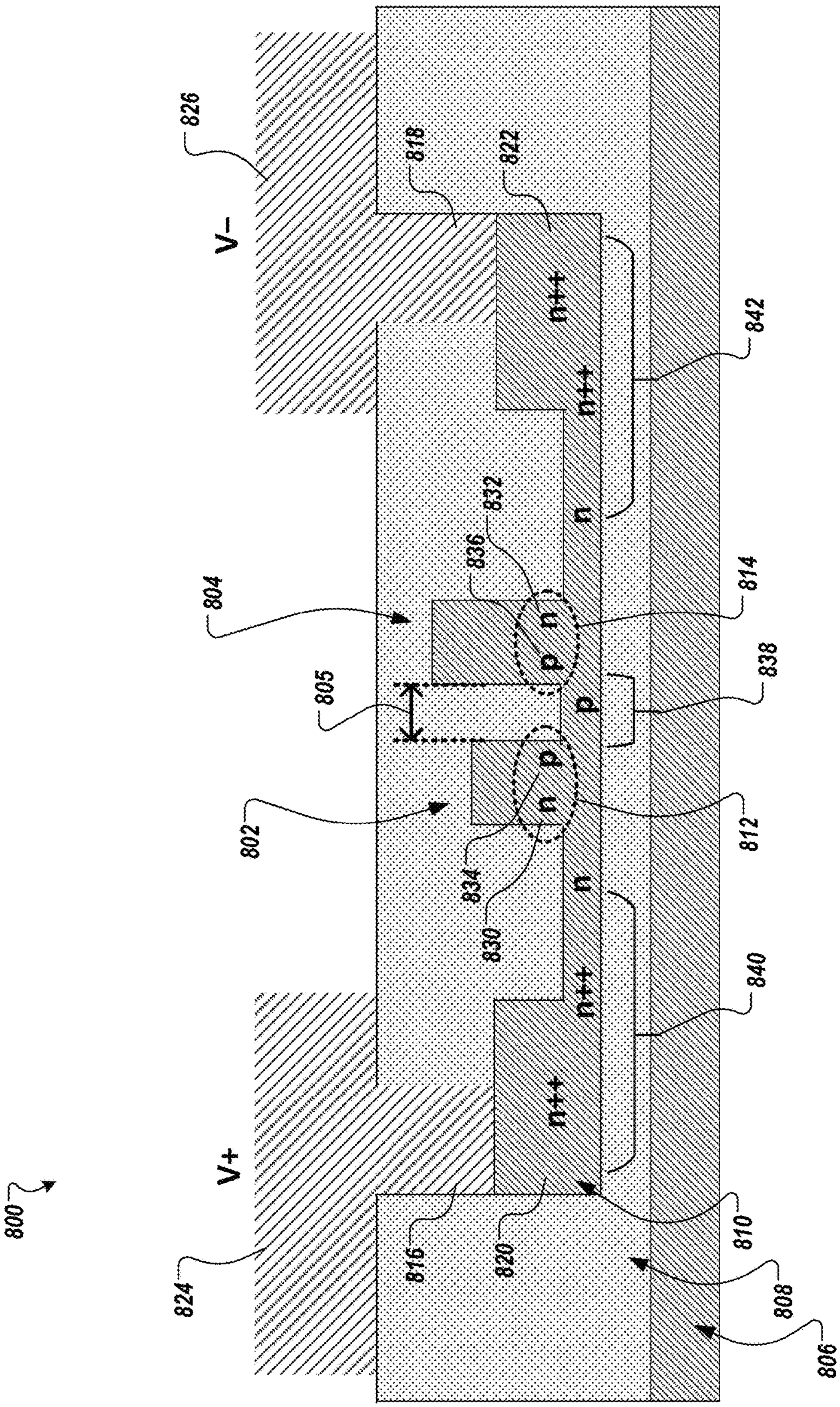
800
V−
V+
n++
n++
n
p
n
p
n
p
n
n++
n++
802
804
805
806
808
810
812
814
816
818
820
822
824
826
830
832
834
836
838
840
842

FIG. 8

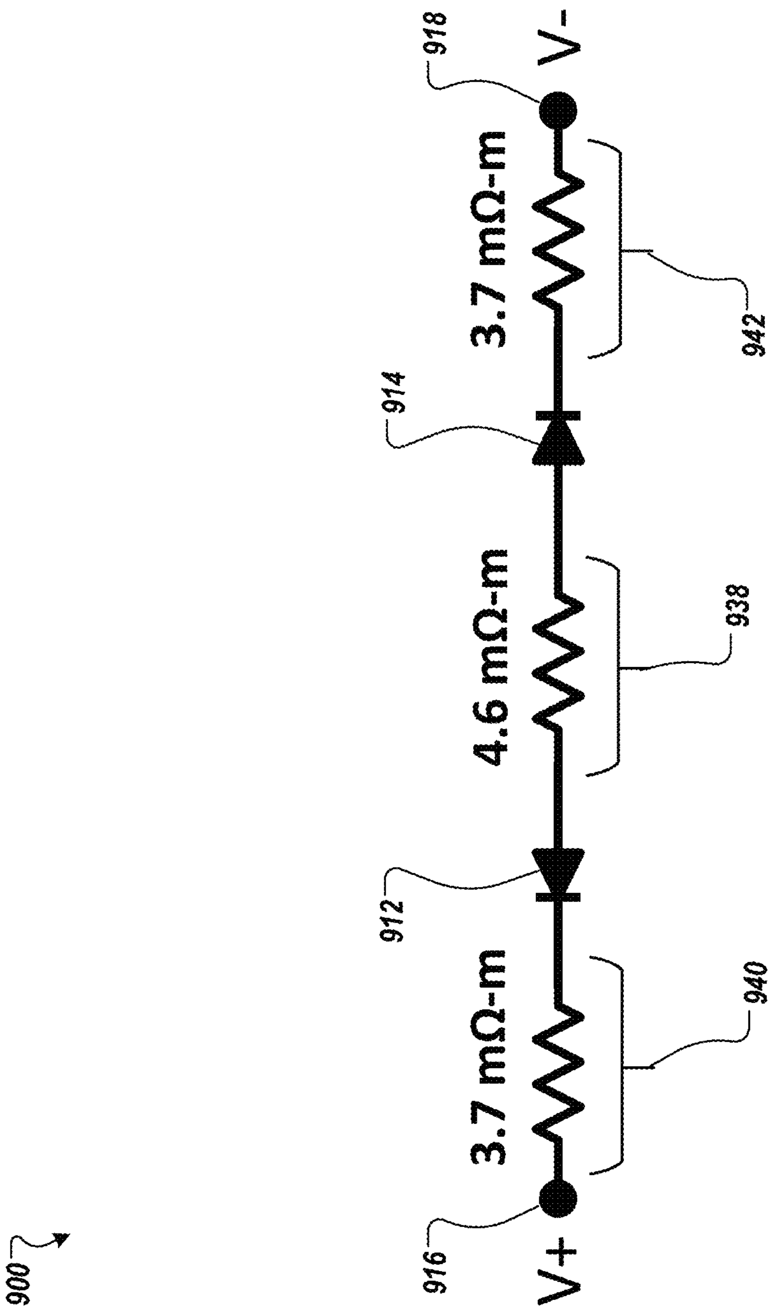

FIG. 9

1000

SPLIT QUASI-TRANSVERSE MODE (TM) POLARIZED LIGHT INTO A FIRST OPTICAL TRANSMISSION PATH AND A SECOND OPTICAL TRANSMISSION PATH 1002

MODULATE A PHASE DIFFERENCE BETWEEN QUASI-TM POLARIZED LIGHT IN THE FIRST OPTICAL TRANSMISSION PATH AND QUASI-TM POLARIZED LIGHT IN THE SECOND OPTICAL TRANSMISSION PATH WITHOUT APPLYING A BIAS VOLTAGE THROUGH AN IMPEDANCE LESS THAN 1 KOHM BETWEEN THE FIRST TRANSMISSION PATH AND THE SECOND OPTICAL TRANSMISSION PATH 1004

COMBINE QUASI-TM POLARIZED LIGHT THAT IS OUTPUT FROM THE FIRST OPTICAL TRANSMISSION PATH AND QUASI-TM POLARIZED LIGHT THAT IS OUTPUT FROM THE SECOND OPTICAL TRANSMISSION PATH 1006

FIG. 10

TRANSVERSE-MAGNETIC POLARIZATION SILICON-PHOTONIC MODULATOR

CROSS-REFERENCE TO RELATED APPLICATIONS

This application is a continuation of U.S. application Ser. No. 17/529,321, filed Nov. 18, 2021, which is incorporated by reference herein in its entirety.

TECHNICAL FIELD

The present disclosure generally relates to electro-optical modulators in silicon photonics.

BACKGROUND

In optical communication systems, electro-optical modulators provide a fundamental mechanism of modulating optical waveforms to carry information. In general, electro-optical modulators operate by modifying one or more properties of optical waveforms according to information, such as digital data, provided by electrical signals.

SUMMARY

Implementations of the present disclosure are generally directed to electro-optical modulators in silicon photonics.

One general aspect includes a silicon-photonic optical modulator including: at least one optical input and at least one optical waveguide that is connected to the at least one optical input. The at least one optical waveguide is configured to propagate quasi-transverse-magnetic (quasi-TM) polarized light, where each of the at least one optical waveguide is configured as a rib waveguide that includes a rib arranged on a slab. The silicon-photonic optical modulator also includes at least one electrode configured to apply at least one electric field to the quasi-TM polarized light in the at least one optical waveguide.

Implementations may include one or more of the following features. The silicon-photonic optical modulator where the silicon-photonic optical modulator is configured as a silicon-photonic depletion modulator in which the at least one optical waveguide includes at least one semiconductor junction diode. The silicon-photonic optical modulator where the at least one electrode is configured to apply the at least one electric field to the quasi-TM polarized light in the at least one semiconductor junction diode. The silicon-photonic optical modulator where an effective refractive index of a TM polarization 2-dimensional (2D) guided mode in the rib waveguide is greater than an effective refractive index of a transverse-electric (TE) polarization 1-dimensional (1-D) guided mode in the slab. The silicon-photonic optical modulator where a doping concentration is increased by more than 10^{17} activated dopants per cm^3 in a first portion of the slab that is within 100 nm of a nearest sidewall of the rib, as compared to a second portion of the slab that is farther than 100 nm from the nearest sidewall of the rib. The silicon-photonic optical modulator where the doping concentration is increased by a value within a range of 5×10^{17} to 1×10^{19} activated dopants per cm^3 in the first portion of the slab that is within a range of 50 nm to 500 nm of the nearest sidewall of the rib, as compared to the second portion of the slab that is farther away from the nearest sidewall of the rib. The silicon-photonic optical modulator, further including a Mach-Zehnder interferometer including the at least one optical waveguide, where the at least one optical waveguide includes: (i) a first optical waveguide including a first semiconductor junction diode, and (ii) a second optical waveguide including a second semiconductor junction diode. The silicon-photonic optical modulator, further including a semiconductor region that connects the first semiconductor junction diode with the second semiconductor junction diode. The silicon-photonic optical modulator where a distance between the first optical waveguide and the second optical waveguide is less than 500 nm for at least a portion of a longitudinal direction of the silicon-photonic optical modulator. The silicon-photonic optical modulator where the first semiconductor junction diode includes a first p-doped region and a first n-doped region. The silicon-photonic optical modulator where the second semiconductor junction diode includes a second p-doped region and a second n-doped region. The silicon-photonic optical modulator where the first p-doped region is connected to the second p-doped region through a third p-doped region in the semiconductor region that connects the first semiconductor junction diode with the second semiconductor junction diode. The silicon-photonic optical modulator where the third p-doped region is configured without any external voltage connection that has an impedance less than 100 ohm.

Another general aspect includes a silicon-photonic optical modulator including: at least one optical input and at least one optical waveguide. The at least one optical waveguide is configured to receive light from the at least one optical input, where each of the at least one optical waveguide is configured as a rib waveguide that includes a rib arranged on a slab. The silicon-photonic optical modulator also includes at least one electrode configured to apply at least one electric field to the light in the at least one optical waveguide. The silicon-photonic optical modulator where a height of the rib waveguide is greater than 0.85 λ/n, where λ is a free-space wavelength of light and n is a refractive index of silicon in the silicon-photonic optical modulator. The silicon-photonic optical modulator where a width of the rib waveguide is greater than a thickness of the slab.

Implementations may include one or more of the following features. The silicon-photonic optical modulator where the height of the rib waveguide is greater than the width of the rib waveguide. The silicon-photonic optical modulator where the height of the rib waveguide is within a range of 320 nm to 500 nm. The silicon-photonic optical modulator where the width of the rib waveguide is within a range of 150 nm to 270 nm. The silicon-photonic optical modulator where the thickness of the slab is within a range of 50 nm to 140 nm. The silicon-photonic optical modulator where for the free-space wavelength of the light equal to 1310 nm: the height of the rib waveguide is within a range of 330 nm to 370 nm. The silicon-photonic optical modulator where the width of the rib waveguide within a range of 200 nm to 240 nm. The silicon-photonic optical modulator where the thickness of the slab is within a range of 70 nm to 110 nm. The silicon-photonic optical modulator where the at least one optical waveguide includes a first rib waveguide and a second rib waveguide. The silicon-photonic optical modulator where a distance between the first rib waveguide and the second rib waveguide is less than 500 nm. The silicon-photonic optical modulator where a height of the first rib waveguide is greater than a height of the second rib waveguide in at least part of the silicon-photonic optical modulator. The silicon-photonic optical modulator where for a first portion of the silicon-photonic optical modulator, the height of the first rib waveguide is greater than the height of the second rib waveguide by at least 40 nm. The silicon-photonic optical modulator where for a second portion of the silicon-photonic optical modulator, the height of the second rib waveguide is greater than the height of the first rib waveguide by at least 40 nm. The silicon-photonic optical modulator where a doping concentration is increased by more than 10^{17} activated dopants per cm^3 in a first portion of the slab that is within 100 nm of a nearest sidewall of the rib, as compared to a second portion of the slab that is farther than 100 nm from the nearest sidewall of the rib.

Another general aspect includes a method of modulating quasi-transverse-magnetic (TM) polarized light, the method including: inputting an input quasi-TM polarized light into at least one optical waveguide, and applying at least one electric field to quasi-TM polarized light in the at least one optical waveguide.

Implementations may include one or more of the following features. The method further including: splitting the input quasi-TM polarized light into a first optical waveguide and a second optical waveguide. The method may also include modulating a phase difference between quasi-TM polarized light in the first optical waveguide and quasi-TM polarized light in the second optical waveguide, without applying a bias voltage through an impedance that is less than 100 ohm between the first optical waveguide and the second optical waveguide. The method may also include combining quasi-TM polarized light that is output from the first optical waveguide and the quasi-TM polarized light that is output from the second optical waveguide. The method where the phase difference between the quasi-TM polarized light in the first optical waveguide and the quasi-TM polarized light in the second optical waveguide is modulated while maintaining finite depletion regions in semiconductor junction diodes in each of the first optical waveguide and the second optical waveguide.

The details of one or more implementations of the subject matter of this disclosure are set forth in the accompanying drawings and the description below. Other features, aspects, and advantages of the subject matter will become apparent from the description, the drawings, and the claims.

BRIEF DESCRIPTION OF THE DRAWINGS

FIG. **1** illustrates an example of a top view of a modulator in which implementations of this disclosure may be utilized;

FIG. **2** illustrates an example of a cross section of a modulator according to implementations of this disclosure;

FIG. **3** illustrates an example of an equivalent circuit along a cross-section of a modulator according to implementations of this disclosure;

FIGS. **4**A and **4**B illustrate examples of a detailed cross section of a single waveguide of a modulator according to implementations of this disclosure;

FIGS. **5**A and **5**B illustrate examples of TE and TM modes in silicon rib waveguides, respectively;

FIG. **6** illustrates an example of a top view of a modulator, according to implementations of the present disclosure;

FIG. **7** illustrates another example of a top view of a modulator, according to implementations of the present disclosure;

FIG. **8** illustrates an example of a cross section of a modulator, according to implementations of the present disclosure;

FIG. **9** illustrates an example of an equivalent circuit along a cross-section of a modulator, according to implementations of the present disclosure; and

FIG. **10** is a flowchart illustrating an example of modulating a TM polarized optical signal, according to implementations of the present disclosure.

DETAILED DESCRIPTION

Systems and techniques are disclosed herein that provide a novel electro-optic modulator in silicon photonics which can achieve a higher bandwidth and/or a lower drive voltage as compared with conventional electro-optical modulators. This is accomplished by novel implementations which reduce the amount of light that leaks into the slab portion of the optical waveguide of the modulator. This enables a higher doping in the slab for the same optical loss, thereby enabling a higher-bandwidth modulator without an increase in the optical loss. These technical advantages are achieved by a modulator structure that enables use of transverse-magnetic (TM) polarized light in the modulator, instead of transverse-electric (TE) polarized light. In some implementations, this is enabled by a rib waveguide structure in which the waveguide height is greater than the waveguide width. This, in turn, results in TM light having a higher effective index than TE light in the rib waveguide.

FIG. **1** illustrates an example of a top view of a differential modulator **100** in which implementations of this disclosure may be utilized. In this example, the modulator **100** is based on a Mach-Zehnder interferometer (MZI) implementation, in which optical signals propagate along the length of the modulator **100** (e.g., from left to right in FIG. **1**) along two optical transmission paths **102** and **104**. At the input of modulator **100**, optical splitter **106** splits an input light into the two optical transmission paths **102** and **104**. At the output of the modulator **100**, the optical combiner **108** combines light output from the two optical transmission paths **102** and **104**. The optical splitter **106** and the optical combiner **108** may be implemented in various ways, for example, using symmetric, asymmetric, or tunable optical intensity couplers. The optical transmission paths **102** and **104** can be implemented by waveguides formed in a semiconducting structure **116**, as described in further detail with reference to FIG. **2**, below. In some implementations, the optical cores of the waveguides, and/or the optical splitter **106**, and/or the optical combiner **108** can include silicon ribs. In some implementations, an optical polarization rotator may be implemented between the input of modulator **100** and the optical transmission paths **102** and **104**, which rotates a polarization of the input light so that quasi-TM light propagates in the optical transmission paths **102** and **104**.

The modulator **100** uses a travelling wave configuration in which voltages applied at terminals **110** and **112** create an electrical signal that propagates along a radio frequency (RF) transmission line **114**, which is terminated at an RF termination resistance. The electrical signal in RF transmission line **114** travels at the same speed as and induces electro-optic modulation in the light that propagates along the two optical transmission paths **102** and **104**. In particular, the RF transmission line **114** is connected to the semiconducting structure **116** via electrodes (described in further detail with reference to FIG. **2**, below), that apply respective voltages, and resulting electric fields, across one or both of the optical transmission paths **102** and **104**. The applied voltage(s) induce a phase shift in the light that propagates in one or both of the optical transmission paths **102** and **104**. In some implementations, the phase shift is differential in that the phase shift magnitude is equal and the phase shift sign is opposite between the optical transmission paths **102** and **104**.

Electro-optic modulation is achieved by varying the voltage at one or both of the terminals **110** and **112** to modulate the differential phase shift between the phase of light in the first optical transmission path **102** and the phase of light in the second optical transmission path **104**. For example, if the terminal voltages are controlled such that the differential phase shift causes destructive interference at the optical combiner **108**, then this corresponds to an "off" or logic "0" state of the modulator **100**. By contrast, if the terminal voltages are controlled such that the differential phase shift between the two optical transmission paths **102** and **104** causes constructive interference at the optical combiner **108**, then this corresponds to the "on" or logic "1" state of the modulator **100**.

The differential phase shift between the two optical transmission paths **102** and **104** can also be influenced by other factors. For example, the physical lengths of the optical transmission paths **102** and **104** can be the same to provide zero inherent differential phase shift, or can be different lengths to provide non-zero inherent differential phase shift. Furthermore, in some implementations, direct current (DC) phase shifters **122** and **124** (e.g., thermo-optic phase-shifters, such as optical waveguide heaters), may be implemented near the ends of the optical transmission paths **102** and **104** to control the relative phases of the two light signals before being combining in the optical combiner **108**.

In some implementations, the phase modulation can be performed by a "push-pull" mechanism, in which the phases of light in both of optical transmission paths **102** and **104** are modulated, to control the relative phase shift between the two paths. In push-pull operation, the voltage V+ at terminal **110** is increased and voltage V− at terminal **112** is decreased (or vice versa), resulting in corresponding phase shifts of light in each of the optical transmission paths **102** and **104**. Push-pull modulation can provide various advantages over non-push-pull modulation, such as achieving smaller average energy consumption and reduced chirp in the modulated signal.

In some scenarios, a direct current (DC) bias connection **118** can be connected between the two optical transmission paths **102** and **104**. The DC bias connection **118** is implemented such that semiconductor junction diodes in each of the optical transmission paths **102** and **104** remain reverse biased, even when data signals applied at the terminals **110** and **112** vary between logical 1 and logical 0. Further details are provided with reference to FIG. **2**, below.

FIG. **2** illustrates an example of a cross section of a modulator **200** (e.g., cross section **126** of the modulator **100** of FIG. **1**).

The cross-section of modulator **200** shows details of the MZI structure. The MZI includes a first optical waveguide **202** and a second optical waveguide **204**. In some implementations, the modulator **200** includes a substrate **206** (e.g., a silicon substrate) an insulating structure **208** (e.g., a dielectric, such as an oxide), and a semiconducting structure **210** (e.g., a silicon layer which includes optical waveguides **202** and **204**).

The optical waveguides **202** and **204** can be implemented, for example, as silicon ribbed waveguides on top of a slab. In the example of FIG. **2**, optical waveguide **202** includes a rib **203** which is arranged on top of a slab **205**. Similarly, optical waveguide **204** includes a rib **207** on top of a slab **209**. The ribs **203**, **207** and the slabs **205**, **209** are all parts of the semiconducting structure **210**. Further details of the ribbed waveguide structure are discussed with reference to FIGS. **4**A and **4**B, below.

Each of the optical waveguides **202** and **204** includes a semiconductor junction. The semiconductor junction diodes can be implemented, for example, by a PIN (P-type/intrinsic/N-type) junction diode or a P/N junction diode. In modulator **200**, a P/N junction is implanted into each of the optical waveguides **202** and **204**, forming a diode in each waveguide. These diodes are shown as first semiconductor junction diode **212** and second semiconductor junction diode **214**.

The modulator **200** also includes electrodes **216** and **218** (e.g., metal electrodes) which are in physical contact with the silicon layer **210**. In some implementations, the electrodes **216** and **218** are in physical contact with P-doped contact regions **220** and **222** of the silicon layer **210**. The electrodes **216** and **218** may be formed, for example, by etching the insulator layer **208** and forming metal (e.g., tungsten, copper, and/or aluminum) contacts. In some implementations, the P-doped regions may instead be N-doped regions, and vice-versa, in modulator **200** (e.g., so that contact regions **220** and **222** are N-doped instead P-doped).

The modulator **200** may also include metal layers **224** and **226** on top of the electrodes **216** and **218**. In some implementations, the metal layers **224** and **226** may form segments of an RF transmission line (e.g., RF transmission line **114** in FIG. **1**).

In some scenarios, a DC bias connection **228** is implemented between the two optical waveguides **202** and **204**. The DC bias connection **228** ensures that the semiconductor junction diodes **212** and **214** remain reverse biased during modulation. For example, in a push-pull mode of modulation, a differential voltage (e.g., V+ and V−) is applied at the metal layers **224** and **226** (and hence at electrodes **216** and **218**). If the voltage (e.g., V+) at first electrode **216** is increased while the voltage (e.g., V−) at the second electrode **218** is decreased, then a width of the depletion region in the first optical waveguide **202** decreases while a width of the depletion region in the second optical waveguide **204** increases (and vice versa). As the depletion widths change, this changes the effective refractive index experienced by the light traveling along each of the optical waveguides **202** and **204**, resulting in corresponding phase shifts of the light. As a result, push-pull modulation can be achieved in the modulator **200**.

In the example of modulator **200**, the DC bias connection **228** is applied at the cathodes **230** and **232** (N-doped regions) of the semiconductor junction diodes **212** and **214**, while the varying voltages V+ and V− are applied at the anodes **234** and **236** (P-doped regions) of the semiconductor junction diodes **212** and **214**. The DC bias connection **228** ensures that the semiconductor junction diodes **212** and **214** remain reverse biased. For example, in the example of modulator **200**, if the bias voltage applied at the DC bias connection **228** is very low (or non-existent), then this may result in activation of the first semiconductor junction diode **212** (e.g., forward bias above approximately 0.6 V for silicon) with a significant number of carriers injected into the depletion region of the first semiconductor junction diode **212**, resulting in forward bias and slower operation. Implementing the DC bias connection **228** with a sufficiently large bias voltage ensures that the semiconductor junction diodes **212** and **214** remain reverse biased under modulation.

FIG. **3** illustrates an example equivalent circuit **300** along a cross-section of a modulator (e.g., the cross section **126** of the modulator **100** of FIG. **1**).

In the example of FIG. **3**, the electrical series resistance **340** between first electrode **316** and first semiconductor junction diode **312** (e.g., corresponding to semiconducting region **240** in FIG. **2**) is denoted R_p (e.g., in units of mΩ-m). The electrical series resistance **342** between second electrode **318** and second semiconductor junction diode **314** (e.g., corresponding to semiconducting region **242** in FIG. **2**) is also denoted R_p (although the actual values of electrical series resistances **340** and **342** may be different, in some implementations). The electrical series resistance **338** between semiconductor junction diodes **312** and **314** (e.g., corresponding to semiconducting region **238** in FIG. **2**) is $2{*}R_n$ (with R_n series resistance between each of semiconductor junction diodes **312** and **314** and DC bias voltage connection **328**).

In the equivalent circuit for the phase modulator shown in FIG. **3**, the resistances R_n and R_p originate primarily from the slab and is the main limitation of the modulator bandwidth. Increasing the doping in the slab reduces the resistance, thus increasing the bandwidth, but it also increases the optical loss, because doped silicon is absorptive.

FIGS. **4**A and **4**B illustrate examples of a detailed cross section of a single waveguide of a silicon-photonic depletion phase modulator (e.g., a waveguide in one of transmission paths **102** or **104** of modulator **100**, or one of waveguides **202** or **204** in FIG. **2**). In particular, FIG. **4**A illustrates an example waveguide **400** configured for TE-polarized light, which may be implemented in some systems, and FIG. **4**B illustrates an example waveguide **420** which is configured for TM-polarized light, according to implementations of the present disclosure.

In both FIGS. **4**A and **4**B, waveguide **400** (and waveguide **420**) is implemented by a rib waveguide structure, with a rib **402** (rib **422**) on top of a slab **404** (slab **424**). Light is guided along the rib **402** (rib **422**) and propagates in a longitudinal direction of the modulator (normal to the cross section shown in FIGS. **4**A and **4**B) by total internal reflection inside the rib **402** (rib **422**). The rib structure allows for a confined optical mode in the rib **402** (rib **422**) while enabling electrical connections to the rib **402** (rib **422**) through the regions on both sides of the slab **404** (slab **424**). As discussed with reference to FIG. **2**, above, phase modulation of light in the rib **402** (rib **422**) is achieved by modulating the voltage difference between the n-doped and p-doped regions of the waveguide **400** (waveguide **420**). For example, increasing the voltage difference between the n-doped and p-doped regions widens the depletion width, thereby increasing the effective refractive index of the optical mode, and allowing for phase modulation of the light in the rib **402** (rib **422**).

The waveguides **400** and **420** in FIGS. **4**A and **4**B differ in several aspects. Most noticeably, the waveguides **400** and **420** differ in dimension, with waveguide **400** (configured for TE-polarized light) being wider and shorter, and waveguide **420** (configured for TM-polarized light) being narrower and taller. The narrower and taller configuration of waveguide **420** in FIG. **4**B enables a reduction in the portion of the optical mode that is in the slab **424**, allowing for a higher doping in the slab **424** for the same optical loss, as compared to waveguide **400** of FIG. **4**A. The higher doping in the slab **424**, in turn, allows for a higher bandwidth in modulator **420**, as compared with modulator **400**, without having to increase the optical loss. This is done by using transverse-magnetic (TM) polarized light in the modulator **420** instead of transverse-electric (TE) polarized light. In practical implementations, the guided optical mode in modulators **400** and **420** is actually a quasi-TE or quasi-TM mode, because guided 2D modes are almost never purely TE or TM modes. In quasi-TM mode, the dominant polarization component of the light is aligned along the y-axis. In quasi-TE mode, the dominant polarization component of the light is aligned along the x-axis. For the sake of brevity in exposition, the word "quasi" may be omitted when discussing the polarization of a guided optical mode in this disclosure.

FIG. **4**A illustrates a cross section of an example waveguide **400** configured for TE-polarized light. The modulator **400** has a rib **402** on top of a slab **404**. The rib has a height **406** (denoted h_{core}) and a width **408** (denoted w_{core}). As shown, in typical implementations of waveguide **400** configured to TE-polarized light, the rib height **406** (h_{core}) is smaller than the rib width **408** (w_{core}). This ensures that the effective index of the TE 2D waveguide mode in the rib **402** is higher than the effective index of the TM 1D slab mode, thus ensuring that a guided TE mode will suffer less leakage to the slab **404**, as compared to a guided TM mode.

There are various reasons for why silicon-photonic modulators, such as modulator **400**, are configured for TE-polarized light.

First, for modulators that employ rib waveguides, the TM 2-D rib mode index is typically significantly lower than the TE 1-D slab mode index. The rib waveguides need special conditions to guide transverse-magnetic (TM) light which are not normally met. This condition is that the effective index of the TM 2-D rib mode must be larger than that of the TE 1-D slab mode. Slab mode means refers to the 1-D mode that would be guided if there is was no rib **402**, and if the slab **404** was infinitely wide. Otherwise, the TM rib mode will be phase matched to the TE slab mode propagating at certain angles with respect to the rib **402**. In such a case, small perturbations will cause the light in the TM mode to leak away into the slab **404**.

Second, TE-polarized light has a tighter vertical confinement in the rib **402**, as compared to TM-polarized light, which mitigates losses due to the substrate below and layers on top. For example, in some implementations, there are metal routing layers above the silicon, and the metal layers can be significantly closer to the silicon before causing significant optical losses for TE-polarized light than TM-polarized light.

Third, in most silicon photonic modulators, the waveguide height **406** is less than the waveguide width **408**, which results in TE-polarized light having a higher effective index than TM-polarized light. This allows for a smaller bend radius, decreasing the size of the silicon photonic devices.

Fourth, most silicon-photonic modulators employ TE-polarized light because most of the other elements in a silicon photonic circuit are designed for TE polarization. For example, most grating couplers are configured for TE polarization.

Fifth, in many scenarios, it is typically easier to fabricate a waveguide structure that has a width greater than its height, e.g., because the lithography process is simplified by a shallower depth of etching.

However, TM polarized light has distinct advantages. For example, TM-polarized light has the advantage of having less light in the slab **424**, as compared to TE-polarized light. To understand why TM-polarized light has less light in the slab **424** than TE-polarized light, one can consider the boundary conditions on the electric field of light that are given by Maxwell's equations. In non-magnetic materials, such as silicon, the transverse electric field, $E_{\parallel}$, is continuous across a boundary; whereas the normal electric field times the permittivity, $(E_{\perp})$ (ε), is continuous across a boundary. Because the permittivity of silicon is approximately 5.8 times than that of oxide, when the electric field is normal to a thin piece of silicon surrounded by oxide, the electric field inside that silicon is approximately 5.8 times lower than in the surrounding oxide. Thus, TM-polarized light has very little electric field inside the silicon slab **424**.

This can be seen visually in FIGS. **5**A and **5**B, which show TE and TM modes in silicon rib waveguides, respectively. FIG. **5**A shows an example of calculated modes of a conventional silicon phase modulator using TE-polarized light. In particular, FIG. **5**A shows the magnitudes of the x-component of the electric field. FIG. **5**B shows an example of calculated modes of a silicon phase modulator using TM-polarized light, according to implementations of the present disclosure. In particular, FIG. **5**B shows the magnitudes of the y-component of the electric field.

As shown, there is significant light in the slab in FIG. **5**A but very little light in the slab in FIG. **5**B. Thus the slab in FIG. **5**B can have significantly higher doping near the rib and thus significantly lower series resistance.

In addition, the waveguide rib dimensions are different in the examples of FIGS. **5**A and **5**B. In both cases, the slab thickness is 90 nm. However, in FIG. **5**A, the waveguide rib height and rib width are 220 nm and 420 nm, respectively, whereas in FIG. **5**B the waveguide rib height and rib width are 400 nm and 220 nm, respectively. The waveguide of FIG. **5**A is a typical modulator waveguide configured for TE-polarized light. As discussed above, in such a configuration, a guided TM mode will leak into the slab, because the effective index of the TM 2D rib mode is lower than the effective index of the TE 1D slab mode (see Table 1, below).

By contrast, the waveguide of FIG. **5**B is able to guide a TM mode without leakage into the slab, because the waveguide rib is taller and narrower. Having a taller waveguide rib increases the effective index of the TM 2D waveguide mode above that of the TE 1D slab mode, as seen in Table 1. This occurs when the waveguide rib height is greater than a threshold of approximately 0.85 λ/n, and when the waveguide rib width is wider than the slab height, where A is the free-space wavelength of light and n is the refractive index of silicon. This guarantees that for TM-polarized light, the electric field has fallen to a low value at the top and bottom of the waveguide so that the boundary condition does not cause significant field to fall outside the waveguide. For instance, for a wavelength of λ=1310 nm, the threshold is 0.85 λ/n=320 nm. Thus, in this example, the waveguide rib height should be larger than 320 nm and the waveguide rib width should be larger than 90 nm.

TABLE 1

Effective mode indices, for a wavelength of λ = 1310 nm.

	Waveguide configured for TE-polarized light (420 × 220 nm^2)	Waveguide configured for TM-polarized light (220 × 400 nm^2)
TE 1D slab (90 nm)	2.25	
TE 2D waveguide	2.70	2.47
TM 2D waveguide	2.13	2.58

Implementations of modulators according to the present disclosure which are configured for TM-polarized light can provide various technical advantages (as compared to typical modulators configured for TE-polarized light). For example, the doping in the slab can be increased significantly and/or higher doping can be placed closer to the rib. In some implementations, a doping concentration can be increased by a value within a range of 5×10^{17} to 1×10^{19} (e.g., increased within a range of 1×10^{18} to 1×10^{19}) activated dopants per cm^3 in a first portion of the slab that is within a range of 50 nm to 500 nm (e.g., 100 nm) of a nearest sidewall of the rib, as compared to a second portion of the slab that is farther than 100 nm from the nearest sidewall of the rib. Some implementations of the present disclosure can provide approximately 3.5 times lower series resistance as compared to a typical modulator that is configured for TE-polarized light. Another advantage is that the phase modulation efficiency can be increased for a given voltage and a given modulator length. This is a consequence of TM-polarized light being more confined horizontally in the waveguide rib, perpendicular to the depletion region, thus resulting in a larger effective index change for a given voltage change.

In addition, modulator implementations according to the present disclosure can be configured to mitigate potential technical challenges. For example, in modulators configured for TM-polarized light, because the waveguide rib is configured to be taller and thinner (as compared with waveguide ribs of typical modulators designed for TE-polarized light), there can be increased series resistance along the vertical edges of the rib, connecting to the top of the waveguide. To mitigate such resistance, a preferred embodiment is to configure the waveguide rib to be only a small amount taller than the threshold to make the effective TM 2D rib index higher than the TE 1D slab effective index. For example, in some implementations, the waveguide rib height is 350 nm and the waveguide rib width is 220 nm, with a 90-nm slab at 1310-nm wavelength.

Another challenge is that the capacitance of the p-n junction of the waveguide (e.g., semiconductor junction diodes **212** and **214** in FIG. **2**) could be increased, as a consequence of the depletion region being taller. However, the fringing fields contribute significantly to the capacitance in these structures, and consequently the capacitance increase is sublinear to the height increase. As such, increasing the waveguide rib height by a factor of 2 results in an increase of the capacitance by only a factor of approximately 1.5.

FIGS. **6**-**9** relate to modulators according to other implementations of the present disclosure. In contrast with the modulators of FIGS. **1**-**3**, the modulators of FIGS. **6**-**9** do not implement any bias voltage connection between the waveguides, resulting in significantly smaller series resistance between electrodes, and thus even higher bandwidth of modulation. Furthermore, in FIGS. **6**-**9**, the modulators implement waveguide structures that vary in height so as to mitigate detrimental optical coupling between the closely-spaced waveguides.

The features described with reference to FIGS. **6**-**9** can help improve upon the structure of the modulators in FIGS. **1**-**3** in various aspects. For example, the presence of DC bias connection **228** in FIG. **2** increases the physical distance of the semiconducting (e.g., silicon) region **238** between the semiconductor junction diodes **212** and **214**. This results in significant electrical series resistance in the semiconducting region **238** that connects the semiconductor junction diodes **212** and **214**. Typical techniques to reduce such electrical series resistance, such as increasing the silicon doping of the semiconducting structure, can have negative consequences such as increasing optical absorption.

Furthermore, the semiconducting regions **240** and **242** in FIG. **2** (which connect each of semiconductor junction diodes **212** and **214** with their respective electrodes **216** and **218**) are P-doped semiconducting material, which has higher resistance than N-doped semiconducting material (for the same optical absorption). This results in significant electrical series resistance in the semiconducting regions **240** and **242** between electrodes **216** and **218** and the semiconductor junction diodes **212** and **214**.

Consequently, the total electrical series resistance between electrodes **216** and **218** in FIG. **2** can significantly attenuate the voltage along the modulator **200** due to charging and discharging of the diode capacitance. Furthermore, this attenuation typically increases as modulation frequency increases. The resulting RF loss along the modulator **200** can detrimentally impact the bandwidth of the modulator **200**.

FIG. **6** illustrates an example of a top view of a modulator **600** according to implementations of the present disclosure.

The modulator **600** is based on an MZI implementation which includes two optical transmission paths **602** and **604**, optical splitter **606**, and optical combiner **608**. The modulator **600** further includes terminals, such as terminal **610** and terminal **612**, through which voltages can be applied. The voltages travel along RF transmission line **614**, which is connected to semiconducting structure **616** via electrodes that apply respective voltages, and resulting electric fields, across one or both of the optical transmission paths **602** and **604**. In some implementations, an optical polarization rotator may be implemented between the input of modulator **600** and the optical transmission paths **602** and **604**, which rotates a polarization of the input light so that quasi-TM light propagates in the optical transmission paths **602** and **604**.

In contrast to the modulator **100** of FIG. **1**, the modulator **600** does not implement any DC bias connection between the two optical transmission paths **602** and **604**. This enables the two optical transmission paths **602** and **604** to be more closely-spaced together, thus reducing electrical series resistance therebetween. For example, in some implementations, the distance between the waveguides of the two optical transmission paths **602** and **604** is less than 0.5 μm for at least a portion of the longitudinal direction of the optical transmission paths **602** and **604**. In some implementations, the distance between the waveguides is less than 2.0 μm for at least a portion of the longitudinal direction of the optical transmission paths **602** and **604**. In some implementations, the distance between the waveguides is within a range of 0.1 μm to 2.0 μm for at least a portion of the longitudinal direction of the optical transmission paths **602** and **604**. In some implementations, the distance between the waveguides is defined as the distance between the inner sidewalls of the two waveguides, at a given point along a longitudinal direction of the modulator **600** (e.g., at a point **605** in FIG. **6**).

However, because the two optical transmission paths **602** and **604** are more closely spaced, there is risk of more significant detrimental optical coupling between light in optical transmission path **602** and light in optical transmission path **604**. To mitigate such optical coupling, in some implementations, the waveguide of one of the optical transmission paths (**602** or **604**) is designed to have a greater height than the other path, at the same distance along the length of the modulator **600**. This helps ensure that the light traveling in the waveguides of optical transmission paths **602** and **604** are not phase matched, thus mitigating optical coupling between the two waveguides. An alternative way to understand the importance of using different waveguide heights is to look at the two eigenmodes of the coupled waveguides of optical transmission paths **602** and **604**. If the waveguides have equal heights, then the lowest order eigenmode is the even eigenmode, and the second lowest eigenmode is the odd eigenmode. In such a scenario, no differential modulation can occur. However, if one waveguide is sufficiently taller than the other, then the lowest order eigenmode consists of light that is predominantly in the taller waveguide, and the second lowest eigenmode is predominantly in the shorter waveguide. This enables differential modulation to occur despite the closely-spaced waveguides. For example, in some implementations, the waveguide of the one of the optical transmission paths **702** or **704** is taller by at least 40 nm than the waveguide of the other optical transmission path. In some implementations, the waveguide height difference is within a range of 40 nm to 120 nm.

Furthermore, in such implementations, the height variation of the two waveguides may be exchanged along the modulator **600**, to help ensure that the total length of the taller portions in each waveguide are equal, and also that the total length of the shorter portions in each waveguide are equal. In the example of FIG. **6**, moving from the left to right, the waveguide of first optical transmission path **602** is taller than the waveguide of the second optical transmission path **604**, and then becomes shorter than the waveguide of the second optical transmission path **604** (alternatively, the first optical transmission path **602** may start shorter and become taller). There may be one such exchange in relative heights in the middle of modulator **600**, but in some implementations, additional height exchanges can be included, e.g., as long as the distance between height exchanges is significantly longer than the beat length between the two eigenmodes in the two waveguides, which is typically 10 μm. This helps mitigate optical coupling between the two waveguides. In some implementations, an odd number of exchanges is preferred, since this will help ensure that the beginning and end transitions cancel each other out.

Although the description of FIG. **6**, above, provided an example of a modulator **600** with variable-height waveguides in the two optical transmission paths **602** and **604**, in other implementations, the waveguides may have constant height along the length of the modulator **600**.

Furthermore, although the description of FIG. **6** provided an example of a modulator **600** without a physical DC bias connection, in some implementations, a DC bias connection may be implemented between the two optical transmission paths **602** and **604**, but through a high impedance. For example, in some implementations, the high impedance is achieved with an impedance greater than 1 kohm. As another example, in some implementations, the high impedance is achieved with an impedance greater than 100 ohm. In such scenarios of a DC bias connection through a high impedance, a current would be generated by the voltage difference between (i) the external voltage and (ii) the voltage that would be between the optical transmission paths **602** and **604** if there were no applied external voltage. This generated current would be less than the diode leakage current plus any photo-generated current in the diodes, and thus the circuit would act primarily as if there were no applied external DC bias voltage (e.g., similar to a true floating voltage). Therefore, it should be appreciated that implementations of the present disclosure, such as those shown in FIGS. **6-9** in which there is no physical DC bias connection, can also be implemented with a DC bias connection but through a high impedance.

The modulator **600** implements an example of a continuous traveling-wave structure, in which the RF transmission line **614** is continuously connected to the semiconducting structure **616**. Alternatively, a segmented traveling-wave structure can be implemented, as described with reference to FIG. **7**, below.

FIG. **7** illustrates another example of a top view of a modulator **700** according to implementations of the present disclosure. The modulator **700** is an example of an implementation of a segmented traveling-wave structure.

The modulator **700** is also based on an MZI implementation which includes two optical transmission paths **702** and **704**, optical splitter **706**, and optical combiner **708**. The modulator **700** further includes terminals, such as terminal **710** and terminal **712**, through which voltages can be applied. The voltages travel along RF transmission line **714**, which is connected to a semiconducting structure **716** via electrodes that apply respective voltages, and resulting electric fields, across one or both of the optical transmission paths **702** and **704**. The modulator **700** also does not implement any DC bias connection between the two optical transmission paths **702** and **704**, which reduces the distance therebetween. For example, in some implementations, the distance between the waveguides of the two optical transmission paths **702** and **704** is less than 0.5 μm for at least a portion of the longitudinal direction of the optical transmission paths **702** and **704**. In some implementations, the distance between the waveguides is less than 2.0 μm for at least a portion of the longitudinal direction of the optical transmission paths **702** and **704**. In some implementations, the distance between the waveguides is within a range of 0.1 μm to 2.0 μm for at least a portion of the longitudinal direction of the optical transmission paths **702** and **704**. In some implementations, the distance between the waveguides is defined as the distance between the inner sidewalls of the two waveguides, at a given point along a longitudinal direction of the modulator **700** (e.g., at a point **705** in FIG. **7**).

The differences between modulator **600** of FIG. **6** and modulator **700** of FIG. **7** arise from the configuration of the semiconducting structure (**616**, **716**) and the manner in which the RF transmission line (**614**, **714**) is connected to the semiconducting structure (**616**, **716**). Modulator **600** of FIG. **6** implements a continuous traveling wave structure in which RF transmission line **614** is continuously directly connected to the semiconducting structure **616**. By contrast, modulator **700** of FIG. **7** implements a segmented traveling wave structure in which RF transmission line **714** is intermittently connected to segments of the semiconducting structure **716**, with intermittent regions **720** along the optical transmission paths **702** and **704** in which there is no semiconducting structure. This structure of modulator **700** can also be referred to as a capacitively loaded traveling wave structure, and has an advantage of providing an additional degree of freedom in implementing the RF transmission **714**, e.g., of the average capacitance per unit length of the RF transmission line **714**. A lumped-element modulator can also benefit from the techniques disclosed herein.

Furthermore, in modulator **700**, the waveguides of optical transmission paths **702** and **704** have different widths in different sections of the modulator **700**, similar to the configuration of the waveguides in modulator **600** of FIG. **6**. Further details of the width variation of the waveguides are provided further below.

FIG. **8** illustrates an example of a cross section of a modulator **800** according to implementations of the present disclosure (e.g., a cross section at point **605** of modulator **600** of FIG. **6** or a cross at point **705** of modulator **700** of FIG. **7**). In particular, the modulator **800** of FIG. **8** is an example of a differential, close-spaced design in which one waveguide is taller than the other.

The cross-section of modulator **800** shows details of the MZI structure. The MZI includes a first optical waveguide **802** and a second optical waveguide **804**. The optical waveguides **802** and **804** can be implemented, for example, as silicon ribbed waveguides on top of a slab. In some implementations, the modulator **800** includes a substrate **806** (e.g., a silicon substrate) an insulating structure **808** (e.g., a dielectric, such as an oxide), and a semiconducting structure **810** (e.g., a silicon layer which includes optical waveguides **802** and **804**).

In some implementations, as discussed in regards to FIGS. **6** and **7**, above, one of the optical waveguides **802** and **804** is taller than the other optical waveguide. For example, in FIG. **8**, the second optical waveguide **804** is taller by at least 40 nm than the first optical waveguide **802**. In some implementations, the waveguide height difference is within a range of 40 nm to 120 nm.

Each of the optical waveguides **802** and **804** includes a semiconductor junction. The semiconductor junction diodes can be implemented, for example, by a PIN (P-type/intrinsic/N-type) junction diode or a P/N junction diode. In modulator **800**, a P/N junction is implanted into each of the optical waveguides **802** and **804**, forming a diode in each waveguide. These diodes are shown as first semiconductor junction diode **812** and second semiconductor junction diode **814**.

The modulator **800** also includes electrodes **816** and **818** (e.g., metal electrodes) which are in physical contact with the silicon layer **810**. In some implementations, the electrodes **816** and **818** are in physical contact with N-doped contact regions **820** and **822** of the silicon layer **810**. The electrodes **816** and **818** may be formed, for example, by etching the insulator layer **808** and forming metal (e.g., tungsten, copper, and/or aluminum) contacts. The modulator **800** may also include metal layers **824** and **826** on top of the electrodes **816** and **818**. In some implementations, the metal layers **824** and **826** may form segments of an RF transmission line (e.g., RF transmission line **114** in FIG. **1**). In some implementations, the P-doped regions may instead be N-doped regions, and vice-versa, in modulator **800** (e.g., so that contact regions **820** and **822** are N-doped instead P-doped).

There are numerous differences between modulator **800** and modulator **200** of FIG. **2**. Most notably, modulator **800** does not implement any DC bias voltage connection between semiconductor junction diodes **812** and **814** (as compared to modulator **200** which implements DC bias connection **228**). Instead, the semiconductor junction diodes **812** and **814** are connected in series with opposite polarity (with anodes **834** and **836** connected together). This ensures that a continuous current can never flow through the semiconductor junction diodes **812** and **814**. This configuration enables the voltages across the two semiconductor junction diodes **812** and **814** to naturally self-adjust to ensure that the diodes **812** and **814** remain reverse-biased, despite variations in modulation voltages (e.g., V+ and V−) that may be applied at electrodes **816** and **818**. Implementing a floating voltage between the semiconductor junction diodes **812** and **814** automatically biases the diodes **812** and **814** at the most efficient point of the modulator in terms of phase shift per volt, which is where the diodes **812** and **814** are just below turn-on. In some implementations, this phase shift per volt is the "gain" of the modulator.

Another difference between modulator **800** and modulator **200** of FIG. **2** is that the polarities of semiconductor junction diodes **812** and **814** are flipped, as compared with modulator **200**. In particular, semiconductor junction diodes **812** and **814** have their respective (P-doped) anodes **834** and **836** closer to the center of modulator **800**, and their respective (N-doped) cathodes **830** and **832** closer to the edges of modulator **800**. As such, the semiconducting region **838** between the semiconductor junction diodes **812** and **814** is P-doped, while semiconducting regions **840** and **842** (connecting each of semiconductor junction diodes **812** and **814** with their respective electrodes **816** and **818**) are N-doped.

These aforementioned differences provide numerous technical advantages for modulator **800**, as compared to modulator **200** of FIG. **2**. One advantage is that the absence of a DC bias voltage connection in modulator **800** enables the two optical waveguides **802** and **804** to be implemented significantly closer to each other, as compared to modulator **200** of FIG. **2**. This enables significant reduction in the size of semiconducting region **838** connecting semiconductor junction diodes **812** and **814**, which significantly reduces the electrical series resistance between semiconductor junction diodes **812** and **814**. For example, in some implementations, the distance (denoted as **805** in FIG. **8**) between the two optical waveguides **802** and **804** is less than 0.5 μm. In some implementations, the distance **805** between the two optical waveguides **802** and **804** is less than 2.0 μm. In some implementations, the distance **805** between the two optical waveguides **802** and **804** is within a range of 0.1 μm to 2.0 μm. In some implementations, the distance **805** between waveguides may be defined as the distance between the inner sidewalls of the two waveguides, at a given point along the longitudinal direction of the modulator **800** (e.g., measured at a cross section of the modulator **800** as shown in FIG. **8**).

Another advantage is that, since P-doped silicon has a higher resistivity than N-doped silicon (for the same optical absorption), higher-resistivity P-doped material is used in the smaller semiconducting region **838** (between semiconductor junction diodes **812** and **814**), and lower-resistivity N-doped material is used in the larger semiconducting regions **840** and **842** (connecting semiconductor junction diodes **812** and **814** with electrodes **816** and **818**). Alternatively, in some implementations, N-doped material can be used in the smaller semiconducting region **838**, and P-doped material can be used in the larger semiconducting regions **840** and **842**.

As a result, the total series resistance between the electrodes **816** and **818** is significantly reduced, thus significantly improving bandwidth and speed of the modulation.

Although the lack of a DC bias voltage connection in modulator **800** takes away a degree of freedom in the ability to adjust the amount of reverse bias in semiconductor junction diodes **812** and **814**, such limitations are, in some scenarios, outweighed by the significant benefits offered by the configuration of modulator **800**, such as improved bandwidth and speed of modulation.

FIG. **9** illustrates an example equivalent circuit **900** along a cross-section of a modulator according to implementations of the present disclosure (e.g., the cross section of modulator **800** of FIG. **8**).

In the example of FIG. **9**, the electrical series resistance **940** between first electrode **916** and first semiconductor junction diode **912** (e.g., corresponding to semiconducting region **840** in FIG. **8**) is 3.7 mΩ-m. The electrical series resistance **942** between second electrode **918** and second semiconductor junction diode **914** (e.g., corresponding to semiconducting region **842** in FIG. **8**) is 3.7 mΩ-m. The electrical series resistance **938** between semiconductor junction diodes **912** and **914** (e.g., corresponding to semiconducting region **838** in FIG. **8**) is 4.6 mΩ-m (without any DC bias voltage connection between the diodes).

As seen in this example, the total series resistance between electrodes **916** and **918** is reduced by about a factor of two, as compared with the equivalent circuit **300** of FIG. **3**. This reduction in total series resistance can significantly improve modulator performance. For example, the modulation bandwidth is increased, by reducing the RF loss along the modulator. Alternatively, modulator efficiency can be improved. For example, a thinner slab can be utilized, which increases total series resistance but also increases optical confinement in the optical waveguides **802** and **804**, thus improving modulator efficiency. Alternatively, a thicker waveguide can be utilized, which increases capacitance but also increases optical confinement.

The modulators according to implementations of the present disclosure can be used in many applications. For example, one application is a high-speed optical intensity modulator to generate intensity-modulated direct-detection (IM-DD) formats such as non-return-to-zero (NRZ) or pulse amplitude modulation (PAM). Another application is to use the modulator in conjunction with a second modulator with a 90-degree relative phase shift as part of a larger interferometer to generate more complex modulation formats for coherent detection, such as quadrature phase-shift keying (QPSK) modulation or quadrature amplitude modulation (QAM). For example, this can be achieved by an in-phase/quadrature (IQ) modulator structure that includes nested modulators, with each of the two branches of a modulator (the outer modulator) implementing another modulator (the inner modulators). In some implementations, phase shifters can be implemented that set 180-degree and 90-degree phase differences for the inner and outer modulators, respectively. Each modulator in such a nested modulator structure can be implemented as described in the present disclosure.

FIG. **10** is a flowchart illustrating an example method **1000** of modulating a quasi-TM polarized optical signal, according to implementations of the present disclosure. The method **1000** may be performed by using a modulator as disclosed herein.

The method **1000** includes splitting quasi-TM polarized light into a first optical transmission path and a second optical transmission path (**1002**). In some implementations, an optical polarization rotator may be implemented at the input of the modulator, which rotates a polarization of the input light so that quasi-TM light propagates in the optical transmission paths.

The method **1000** further includes modulating a phase difference between quasi-TM polarized light in the first optical transmission path and quasi-TM polarized light in the second optical transmission path without applying a bias voltage between the first optical transmission path and the second optical transmission path (**1004**). In some implementations, the phase difference between the quasi-TM polarized light in the first optical transmission path and the quasi-TM polarized light in the second optical transmission path is modulated while maintaining finite depletion regions in semiconductor junction diodes in each of the first optical transmission path and the second optical transmission path. For example, this modulation can be performed using the floating anode structure of modulators discussed above.

The method **1000** further includes combining quasi-TM polarized light that is output from the first optical transmission path and quasi-TM polarized light that is output from the second optical transmission path (**1006**).

While this disclosure contains many specific implementation details, these should not be construed as limitations on the scope of any invention or of what may be claimed, but rather as descriptions of features that may be specific to particular implementations of particular inventions. Certain features that are described in this disclosure in the context of separate implementations can also be implemented in combination in a single implementation. Conversely, various features that are described in the context of a single implementation can also be implemented in multiple implementations separately or in any suitable subcombination. Moreover, although features may be described above as acting in certain combinations and even initially claimed as such, one or more features from a claimed combination can in some cases be excised from the combination, and the claimed combination may be directed to a subcombination or variation of a subcombination.

Similarly, while operations are depicted in the drawings in a particular order, this should not be understood as requiring that such operations be performed in the particular order shown or in sequential order, or that all illustrated operations be performed, to achieve desirable results.

What is claimed is:

1. A silicon-photonic optical modulator comprising:

at least one optical input;

a Mach-Zehnder interferometer comprising a first optical waveguide and a second optical waveguide that are connected to the at least one optical input and that are configured to propagate quasi-transverse-magnetic (quasi-TM) polarized light, wherein each of the first optical waveguide and the second optical waveguide is configured as a rib waveguide that comprises a rib arranged on a slab;

a polarization rotator between the at least one optical input and the first optical waveguide, the polarization rotator configured to rotate a polarization of input light from the at least one optical input to produce the quasi-TM polarized light in the first optical waveguide; and

electrodes configured to apply electric fields to the quasi-TM polarized light.

2. The silicon-photonic optical modulator of claim **1**, wherein the silicon-photonic optical modulator is configured as a silicon-photonic depletion modulator in which the first optical waveguide and the second optical waveguide each comprise a semiconductor junction diode, and

wherein the electrodes are configured to apply the electric fields to the quasi-TM polarized light in the semiconductor junction diodes of the first optical waveguide and the second optical waveguide.

3. The silicon-photonic optical modulator of claim **1**, wherein an effective refractive index of a TM-polarization 2-dimensional (2D) guided mode in the rib waveguide of each of the first optical waveguide and the second optical waveguide is greater than an effective refractive index of a transverse-electric (TE) polarization 1-dimensional (1-D) guided mode in the slab.

4. The silicon-photonic optical modulator of claim **1**, wherein a height of the rib of each of the first optical waveguide and the second optical waveguide is greater than 0.85 λ/n, where λ is a free-space wavelength of light and n is a refractive index of silicon in the silicon-photonic optical modulator, and

wherein a width of the rib is greater than a thickness of the slab.

5. The silicon-photonic optical modulator of claim **1**, wherein a height of the rib of each of the first optical waveguide and the second optical waveguide is greater than 320 nm.

6. The silicon-photonic optical modulator of claim **1**, wherein the first optical waveguide comprises a first rib waveguide comprising a first semiconductor junction diode, and the second optical waveguide comprises a second rib waveguide comprising a second semiconductor junction diode,

wherein the first semiconductor junction diode and the second semiconductor junction diode are electrically connected by a semiconductor region, and

wherein the semiconductor region is configured without any external voltage connection that has an impedance less than 100 ohm.

7. The silicon-photonic optical modulator of claim **1**, comprising a segmented electrode structure comprising:

as the electrodes, a plurality of electrode segments spaced apart along a longitudinal direction of the Mach-Zehnder interferometer, the plurality of electrode segments configured to apply the electric fields to the quasi-TM polarized light; and

a plurality of intermittent regions at which the first optical waveguide and the second optical waveguide are free of applied electric fields.

8. The silicon-photonic optical modulator of claim **1**, wherein a distance between the first optical waveguide and the second optical waveguide is less than 2.0 μm for at least a portion of a longitudinal direction of the Mach-Zehnder interferometer.

9. The silicon-photonic optical modulator of claim **1**, wherein the first optical waveguide comprises a first semiconductor junction diode and the second optical waveguide comprises a second semiconductor junction diode, and

wherein the first semiconductor junction diode and the second semiconductor junction diode are connected in series with opposite polarity.

10. The silicon-photonic optical modulator of claim **1**, wherein quasi-TM light traveling in the first optical waveguide is phase-mismatched with quasi-TM light traveling in the second optical waveguide.

11. The silicon-photonic optical modulator of claim **1**, wherein the first optical waveguide comprises a first rib extending from the slab and the second optical waveguide comprises a second rib extending from the slab,

wherein a height of the first rib is greater than a height of the second rib.

12. The silicon-photonic optical modulator of claim **11**, wherein the height of the first rib is greater than the height of the second rib by a difference in a range from 40 nm to 120 nm.

13. The silicon-photonic optical modulator of claim **11**, wherein the height of the first rib is greater than the height of the second rib at a same first distance along the first optical waveguide and the second optical waveguide, and

wherein a second height of the second rib is greater than a second height of the first rib at a same second distance along the first optical waveguide and the second optical waveguide.

14. The silicon-photonic optical modulator of claim **11**, wherein the first optical waveguide and the second optical waveguide exchange, an odd number of times, which of the first rib or the second rib is taller along lengths of the first optical waveguide and the second optical waveguide.

15. A silicon-photonic optical modulator comprising:

at least one optical input;

a Mach-Zehnder interferometer comprising a first rib waveguide and a second rib waveguide that are connected to the at least one optical input, wherein the first rib waveguide comprises a first rib extending from a slab, wherein the second rib waveguide comprises a second rib extending from the slab, and wherein the first rib waveguide and the second rib waveguide are configured to propagate quasi-transverse-magnetic (quasi-TM) polarized light;

a polarization rotator between the at least one optical input and the first rib waveguide, the polarization rotator configured to rotate a polarization of input light from the at least one optical input to produce the quasi-TM polarized light in the first rib waveguide; and

electrodes configured to apply electric fields to light in at least one of the first rib waveguide or the second rib waveguide,

wherein the first rib waveguide comprises a first semiconductor junction diode and the second rib waveguide comprises a second semiconductor junction diode,

wherein a height of the first rib waveguide and a height of the second rib waveguide are greater than 0.85 λ/n, where λ is a free-space wavelength of light and n is a refractive index of silicon in the silicon-photonic optical modulator.

16. The silicon-photonic optical modulator of claim **15**, wherein a width of the first rib is greater than a thickness of the slab.

17. The silicon-photonic optical modulator of claim **15**, wherein the height of the first rib waveguide is in a range from 320 nm to 500 nm, and wherein a thickness of the slab is in a range from 50 nm to 140 nm.

18. The silicon-photonic optical modulator of claim **17**, wherein the height of the first rib waveguide is in a range from 330 nm to 370 nm, and wherein the thickness of the slab is in a range from 70 nm to 110 nm.

19. The silicon-photonic optical modulator of claim **15**, comprising a segmented electrode structure comprising:

as the electrodes, a plurality of electrode segments spaced apart along a longitudinal direction of the Mach-Zehnder interferometer, the plurality of electrode segments configured to apply the electric fields to the quasi-TM polarized light; and

a plurality of intermittent regions at which the first rib waveguide and the second rib waveguide are free of applied electric fields.

20. The silicon-photonic optical modulator of claim **15**, wherein a height of the first rib is greater than a height of the second rib.

* * * * *